VOLUME 33 NUMBER 3

ACCOUNTS of CHEMICAL RESEARCH®

MARCH 2000

Doped Rare Gas Solids as Model Systems for Chromophore−Matrix Interactions

PETER GEISSINGER,*,† THOMAS GIERING,* WOLFGANG RICHTER, AND DIETRICH HAARER

Institute of Physics and BIMF, University of Bayreuth, D-95440 Bayreuth, Germany

Received February 5, 1998

ABSTRACT

Molecular electronic states are extremely sensitive to changes in their environment. Therefore, by inserting probe molecules into a host material and monitoring the ensuing changes in the widths and spectral positions of the electronic absorption bands, interactions of probe and host molecules can be studied. A statistical mechanical model used to analyze these data can also be employed to extract from pressure-induced changes of the band shape information about the local environment of the probe molecule. Dye-doped solid rare gases are ideal model systems to test the basic assumptions of the statistical model, revealing its potential and limitations.

1. Introduction

A useful procedure for the study of intermolecular interactions in the condensed phase is to insert into the system of interest small concentrations of a different molecular species as probes. If the guest or probe molecule is chosen such that its optical absorption does not interfere with that of the host molecules, it is possible to address experimentally only the electronic states of the guest molecule, obtaining truly local information. Even though only the optical absorption of the guest molecule is studied experimentally, its electronic state energies reflect the influence of the host material. Electrostatic and/or dispersive guest/host interactions will shift the electronic transition energies with respect to their values in the gas phase. Furthermore, strain fields can lead to changes in the geometry of the guest molecules, which, in turn, changes the electronic state energies as well.[1]

Not only are the spectral positions of the optical absorption lines of the guest molecules affected, but also their widths. The reason is that the host material contains additional excitation modes (like lattice phonons), which couple to the guest electronic states. These dynamic effects are especially prominent in disordered host materials, where low-energy excitations such as two-level tunneling systems (TLS)[2] and (pseudo) local modes[3] provide relaxation channels, thereby leading to an increase in homogeneous absorption line widths. Therefore, measuring the electronic transition energies of guest molecules provides information on the guest−host interaction strength (via the line shift) and about dynamical processes in the guest/host system (via the line widths).

The strength of the guest/host interaction depends on the local site geometry, that is, on the arrangement of the host molecules within the interaction range of the guest molecules. If the local structure were unique, that is, if each of the guest molecules had exactly the same microscopic local environment, all guest molecules would experience exactly the same shift of their electronic state energies. In reality, however, a distribution of local environments exists, which, in turn, leads to a distribution of state energies. Since the electronic states corresponding to the optical transition under study respond differently

Peter Geissinger received a Ph.D. in experimental physics from the University of Bayreuth, Germany, in 1994. In 1998 he joined the University of Wisconsin−Milwaukee as Assistant Professor of Chemistry. His research interests focus on using high-resolution laser spectroscopy to investigate intermolecular interactions in solids.

Thomas Giering studied physics at the University of Bayreuth. In 1997 he obtained a Ph.D. in experimental physics for investigations of cryogenic matrices with high-resolution laser spectroscopy. Since then he has been working in the Research & Development Department of Giesecke & Devrient, Germany.

Wolfgang Richter obtained a Ph.D. from the University of Würzburg in 1979. Since 1981 he has been working as a senior scientist in the group of Prof. Haarer, Bayreuth. His main interest is in the field of high-resolution spectroscopy of organic and inorganic glasses.

Dietrich Haarer currently holds a chair in experimental physics at the University of Bayreuth. His particular fields of research are laser spectroscopy, optical and photoelectric properties of polymers, holography, and optical storage devices. In 1992 he shared a Max-Planck-Prize with Prof. Silbey, MIT.

* To whom correspondence should be addressed. Phone: +49 921 55-3235. Fax: +49 921 55-3250.

† Present address: Department of Chemistry, University of Wisconsin−Milwaukee, P.O. Box 413, Milwaukee, WI 53201-0413.

10.1021/ar980011l CCC: $19.00
Published on Web 01/27/2000

to the slight variations in the environment, inhomogeneous broadening will be observed. In other words, the inhomogeneous line shape consists of a large number of homogeneous absorption lines that are shifted with respect to each other.

While inhomogeneous broadening masks the homogeneous line shapes (the ratio of inhomogeneous to homogeneous widths can exceed 10^5), it provides nevertheless valuable information on guest/host interactions when analyzed with a statistical mechanical model.[4,5] This model and its derivatives were widely applied to porphyrin- and phthalocyanine-type guest molecules in host materials ranging from alcohol glasses[6] to biopolymers[7] and aerogels,[8] even though these systems satisfy the basic assumption of the model rather poorly. For example, the statistical model assumes that the host material can be dissected into spherical matrix units, which interact pairwise with the guest molecule through a purely dispersive interaction.[5] For polymer hosts, for example, the matrix units were usually chosen to be the monomer units.[9] Our goal was to investigate systems that closely match the assumptions of the model. We chose solid rare gases as host matrices, with each rare gas atom being equivalent to one matrix unit. To facilitate comparison with previous experiments, we also used free base phthalocyanine (H_2Pc) as guest molecule.

The question arises whether the local environment of H_2Pc in solid rare gases is crystalline, amorphous, or disordered. It is known that solid rare gases, which are quench condensed at liquid helium temperatures, exhibit a nanocrystalline structure, with grain sizes of the order of 10 nm and densities that are up to 35% less than the densities in corresponding bulk crystals.[10] Due to the large number of randomly sized and oriented crystallites, the atoms in the regions between the crystallites show a wide distribution of interatomic spacings.[11] Therefore, it was proposed that the interfacial component consists of a solid-state structure without long- or short-range order.[12] This was confirmed by X-ray diffraction experiments on nanocrystalline metals with similar grain sizes: the probability function for interatomic distances was found to be gaslike (that is, a step function).[12] For energetic reasons the assumption that the guest molecule is located between the crystallites in the low-density region of host is reasonable.

This assumption can be tested experimentally by measuring and comparing homogeneous and inhomogeneous widths of a specific electronic transition of a guest molecule in different hosts.[13,14] Additional information comes from the analysis of the effects of external hydrostatic pressure on the optical transitions: from the measured pressure-induced line shifts the compressibility of the local environment of the guest molecule can be extracted.[9,15,16] Since the free volume that is available to the guest molecule influences the "local" compressibility, structural information can be obtained. As will be shown below, the same statistical model that we set out to apply to these model systems can also be used to extract local compressibilities from the observed pressure shifts. Further information on local environments and their impact on homogeneous and inhomogeneous widths can be gained if structural changes are induced in a controlled fashion. This is, indeed, possible with quench-condensed rare gas mixtures, which for certain mixing ratios exhibit an amorphous structure instead of a nanocrystalline structure.[17]

While measuring inhomogeneous line shapes is straightforward, determining the homogeneous line shapes requires a line narrowing technique that allows for the extraction of the homogeneous widths from the inhomogeneously broadened absorption band. One method to accomplish this is the hole-burning technique,[18,19] which requires the use of guest molecules that can undergo a phototransformation upon electronic excitation. Using a narrow band laser, only guest molecules are excited whose homogeneous absorption lines overlap with the laser profile. Therefore, only these molecules are phototransformed. If the photoproduct absorbs in a different spectral region, a dip in the absorption band is created, which is called a spectral hole. Ideally, the width of the spectral hole is twice the homogeneous width.[20] The spectral hole also serves as a narrow frequency marker, which responds with high sensitivity to external perturbations such as the application of hydrostatic pressure. Performing pressure experiments on spectral holes rather than the entire inhomogeneous absorption line is advantageous, as the pressures required to induce measurable changes of the profiles of spectral holes are several orders of magnitude smaller.

The goals of this study are twofold: first, as described above, we want to test statistical models by applying them to systems that meet the basic theoretical assumptions, and second, we want to extract structural information about the local environments. The paper is structured as follows: after the statistical model is highlighted, inhomogeneous line shapes and pressure-shifted spectral holes are analyzed to show the influence of correlations between matrix units on interaction parameters and on matrix compressibilities. The last section describes the homogeneous line widths of H_2Pc in solid rare gases and rare gas mixtures.

2. Statistical Model

The observed inhomogeneous absorption band is the convolution of the homogeneous line shape $\Gamma(\nu)$ and the inhomogeneous distribution function $I(\nu)$. For the case of a guest molecule (the "solute") interacting with N matrix units (the "solvent"), the latter can be written as[4,5,9,21]

$$I(\nu) = \frac{1}{V^N} \int \mathrm{d}\vec{R}_1 \cdots \mathrm{d}\vec{R}_N P(\vec{R}_1, ..., \vec{R}_N) \delta(\nu - \sum_{i=1}^{N} \nu(\vec{R}_i)) \quad (1)$$

where V is the sample volume and $P(\vec{R}_1, ..., \vec{R}_N)$ is the $N+1$ particle distribution function describing the probability for a certain arrangement of the guest molecule and N surrounding matrix units. A matrix unit at position $\vec{R}_i$ with respect to the guest molecule will shift the electronic

absorption line of the dye molecule by some amount $\nu(\vec{R}_i)$. The contributions of all matrix units are assumed to be additive. Averaging over all possible configurations $(\vec{R}_1, ..., \vec{R}_N)$ yields $I(\nu)$.

The function $\nu(\vec{R})$, which describes the shift of the guest electronic *transition* energy, is given by the difference of the interaction potentials of a matrix unit with the guest in the excited and ground states, respectively. Assuming that the locations $\vec{R}_{\min}$ of the minima of the ground- and excited-state interaction potentials are identical and considering only nonpolar solute and solvent molecules and atoms, $\nu(\vec{R})$ is of the familiar Lennard-Jones type,

$$\nu(\vec{R}) = \begin{cases} 4\epsilon\left[\left(\frac{\sigma}{R-R_0}\right)^{12} - \left(\frac{\sigma}{R-R_0}\right)^{6}\right] & \text{if} \quad R \geq R_0 \\ \infty & \text{if} \quad R < R_0 \end{cases} \quad (2)$$

with the origin shifted by R_0 to account for the large size difference between solute and solvent.[5] In this representation, $R_0 + \sigma/2$ is the solute radius,[5] while $2^{1/6}\sigma$ can be taken as the solvent diameter. ϵ is the *difference* of the respective depths of the excited-state and ground-state interaction potentials.

The further evaluation of eq 1 using Fourier representions and cumulant expansions has been described elsewhere.[5,22,23] For large number densities ρ of matrix units around the guest molecule ($\rho \rightarrow \infty$), this leads to a Gaussian inhomogeneous distribution,

$$I(\nu) = \frac{1}{\sqrt{2\pi\sigma_s^2}} \exp\left[-\frac{(\nu - \nu_s)^2}{2\sigma_s^2}\right] \quad (3)$$

The experimentally observable quantities solvent shift ν_s (which is the spectral position of the band maximum with respect to the gas-phase position) and full width of the Gaussian distribution at half-maximum, $\Gamma_s = 2(2 \ln 2)^{1/2}\sigma_s$ are related to the local number density ρ of the matrix units and to the energy-shift function $\nu(\vec{R})$:

$$\nu_s = \rho \int \mathrm{d}\vec{R}\, g(\vec{R})\nu(\vec{R}) \quad (4)$$

$$\sigma_s^2 = \rho \int \mathrm{d}\vec{R}\, g(\vec{R})\nu(\vec{R})^2 + \rho^2 \int\int \mathrm{d}\vec{R}\, \mathrm{d}\vec{R}'[g_3(\vec{R},\vec{R}') - g(\vec{R})g(\vec{R}')]\nu(\vec{R})\nu(\vec{R}') \quad (5)$$

The function $g_3(\vec{R},\vec{R}')$ in eq 5 is a three-particle distribution function describing the probability for a certain arrangement of guest molecule and *two* matrix units. Therefore, $g_3(\vec{R},\vec{R}')$ contains correlations between matrix units. If these correlations are neglected, which is equivalent to neglecting the mutual steric exclusion of the matrix units, $g_3(\vec{R},\vec{R}')$ can be written as the product of two two-particle distribution functions $g(\vec{R})$ (guest molecule + one matrix unit):[5,24]

$$g_3(\vec{R},\vec{R}') = g(\vec{R})g(\vec{R}') \quad (6)$$

In this case, the term proportional to ρ^2 in eq 5 vanishes. The factorization (eq 6) is valid in the limit of small number densities $\rho \rightarrow 0$ of matrix units, in contradiction with the earlier assumption of $\rho \rightarrow \infty$. Matrix correlations can be included by writing $g_3(\vec{R},\vec{R}')$ as the product of the solvent−solute distribution functions $g(\vec{R})$ and $g(\vec{R}')$ and a solvent−solvent distribution function $g_s(|\vec{R} - \vec{R}'|)$:[22,23,25]

$$g_3(\vec{R},\vec{R}') \approx g(\vec{R})g(\vec{R}')g_s(|\vec{R} - \vec{R}'|) \quad (7)$$

The simplest choice for $g(\vec{R})$ is a step function that excludes the volume of the guest molecule (which is assumed to be enclosed in a spherical cavity with radius $R_0 + R_c$) as a possible location for a matrix unit:

$$g(\vec{R}) = \begin{cases} 1 & \text{if} \quad R \geq R_0 + R_c \\ 0 & \text{if} \quad R < R_0 + R_c \end{cases} \quad (8)$$

R_c determines how close a matrix unit can come to the guest molecule. Similarly, we choose a step function for the solvent−solvent distribution $g_s(|\vec{R} - \vec{R}'|)$, meaning that a matrix unit (with diameter $2^{1/6}\sigma$) can be found anywhere with equal probability except within the volume occupied by another matrix unit:

$$g_s(|\vec{R} - \vec{R}'|) = \begin{cases} 1 & \text{if} \quad |\vec{R} - \vec{R}'| \geq 2^{1/6}\sigma \\ 0 & \text{if} \quad |\vec{R} - \vec{R}'| < 2^{1/6}\sigma \end{cases} \quad (9)$$

For polymeric matrices the parameters R_0, R_c, and σ are ill-defined and, therefore, in earlier studies were extracted from additional experimental data.[9] The geometric simplicity of rare gases, however, allows one to determine these parameters beforehand: the Lennard-Jones parameters σ of pure solid rare gases (see Table 2, below) come from literature data,[26] while the cutoff $R_0 + R_c$ is given by the sum of solute and solvent radii $R_0 + (1 + 2^{1/6})\sigma/2$. Finally, R_0 can be estimated from the solute radius $R_F = R_0 + \sigma/2$. With these parameters we can calculate exclusively from the measured inhomogeneous line shapes the number density ρ of matrix units surrounding the guest molecule and the interaction potential parameter ϵ with and without consideration of matrix correlations.

As mentioned in the Introduction, the statistical mechanical approach also provides a description of the effects of external pressure on spectral holes.[9] In our experiments the pressure change is always accompanied by a simultaneous change in temperature (see Experimental Details). Therefore, the observed hole shifts will be due not only to pressure changes but also to the thermal expansion of the matrix. We have extended the statistical model to account for temperature effects as well.[24]

In analogy to the inhomogeneous distribution (eq 1), the temperature/pressure kernel, i.e., the probability that a dye molecule with the original solvent shift ν will have a new transition frequency ν' after a pressure change Δp and a temperature change ΔT, can be written as

$$f(\nu'|\nu,\Delta p,\Delta T) = \frac{1}{I(\nu)V^N}\int \mathrm{d}\vec{R}_1 \cdots \mathrm{d}\vec{R}_N P(\vec{R}_1, ..., \vec{R}_N)\delta(\nu - \sum_{i=1}^{N}\nu(\vec{R}_i))\delta(\nu' - \sum_{i=1}^{N}\nu'(\vec{R}_i,\Delta p,\Delta T)) \quad (10)$$

For the small pressure changes in our experiments, the temperature/pressure shift was found to be linear. It is assumed, that—in analogy to pure pressure effects[9]—the hole shift and the hole broadening due to the thermal expansion are linear functions of the temperature change. The function $\nu'(\vec{R},\Delta p,\Delta T)$ can then be linearized to

$$\nu'(\vec{R},\Delta p,\Delta T) = \nu(\vec{R}) - \kappa\left(\frac{\partial\nu(\vec{R})}{\partial R}\frac{R}{3}\right)\Delta p + \gamma\left(\frac{\partial\nu(\vec{R})}{\partial R}\frac{R}{3}\right)\Delta T \quad (11)$$

The contributions from pressure and temperature changes have opposite signs and are proportional to the gradient $\partial\nu(\vec{R})/\partial R$ of the transition energy shift function as well as to the compressibility κ of the matrix and its volume thermal expansion coefficient γ, respectively. If the thermal expansion of the matrix is known, eq 11 can be used to determine the compressibility κ of the host matrix from the measured line or hole shifts $\Delta\nu(\nu,\Delta p,\Delta T) = \nu'(\vec{R},\Delta p,\Delta T) - \nu(\vec{R})$. To study whether the consideration of matrix correlations affects the calculated compressibility, we included correlation effects in the evaluation of eq 10 (details in ref 24). The calculation leads to expressions for the pressure/temperature shift that contain integrals that are similar to those in eqs 4 and 5. For the transition energy shift function (2), these integrals have to be evaluated numerically, to extract the compressibility from experimental data. It is possible, however, to obtain an analytical expression for the pressure/temperature shift $\Delta\nu(\nu,\Delta p,\Delta T)$ if a purely attractive van der Waals potential $\nu(\vec{R}) \propto 1/R^6$ is employed:

$$\Delta\nu(\nu,\Delta p,\Delta T) = 2\nu[\kappa\Delta p - \gamma\Delta T] \quad (12)$$

This result holds irrespective of the inclusion of matrix correlations in the analysis, suggesting that, for the determination of the compressibility κ, correlations between matrix units will also play a minor role if the transition energy shift function (eq 2), which is based on a Lennard-Jones potential, is used. To verify this assumption the measured pressure/temperature shifts will be evaluated numerically using the Lennard-Jones-based potential and analytically using eq 12.

3. Experimental Details

For our experiments, rare gases (Linde) with a purity of 99.998% (argon) and 99.990% (krypton and xenon) were used. The gases either were used directly or were mixed prior to further processing. The concentrations of the gas mixtures were determined by monitoring the pressure in the mixing chamber during the composition process. As guest molecule, free base phthalocyanine (H_2Pc) (Aldrich) was used. To produce solid matrices doped with low concentrations of guest molecules the latter were evaporated in a Knudsen effusion furnace ($T \approx 600$ K). After being homogenized with the matrix gas in a superheating chamber, the mixture passed through a nozzle onto a sapphire substrate, which was mounted on the coldfinger of a continuous flow cryostat. The samples were prepared in vacuo. In a typical sample with a thickness of about 10 μm, the H_2Pc concentration was approximately 2×10^{-3} mol/L. To attain temperatures down to 1.5 K and to maximize the cooling efficiency, the solid matrices were immersed into liquid helium after preparation. Pumping on the helium bath lowered the temperature. Sealing off the helium bath produced the desired hydrostatic pressure changes but also led to temperature changes according to the vapor pressure curve.

Broadband absorption spectra were recorded with a monochromator (Jobin-Yvon THR 1500, spectral resolution ~0.2 cm^{-1}). Spectral holes were burnt and scanned with a single-mode dye laser system (Coherent 599, spectral width ~3 MHz; for details see ref 27). Spectral hole formation is achieved by a light-induced 90° rotation of the two inner protons of H_2Pc.

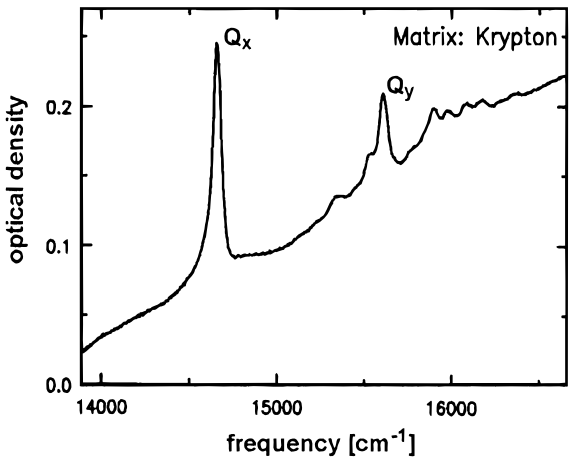

FIGURE 1. Absorption spectrum of H_2Pc in a krypton matrix.

Table 1. Center Frequency ν_c, fwhm Γ_s, and Solvent Shift ν_s of the Q_x Band of H_2Pc in Solid Rare Gases at $T = 4$ K

matrix	ν_c (Q_x) (cm^{-1})	Γ_s (Q_x) (cm^{-1})	ν_s (Q_x) (cm^{-1})
argon	14 764	44	364
krypton	14 664	58	464
xenon	14 540	89	593

4. Inhomogeneous Distribution and Correlation Effects

Figure 1 shows a low-temperature ($T = 4$ K) absorption spectrum of H_2Pc in solid krypton. We are interested in the absorption band labeled Q_x, which corresponds to the lowest energy electronic transition of H_2Pc. This transition shows large inhomogeneous broadening—for example, in a krypton matrix at $T = 4$ K the ratio of inhomogeneous to homogeneous width is roughly 1500! Table 1 summarizes for all investigated rare gases the measured center frequencies $\nu_c(Q_x)$, the full widths at half-maximum

Table 2. Calculated Number Densities and Potential Parameters with ($\hat{\rho}$,$\hat{\epsilon}$) and without (ρ,ϵ) Matrix Correlations[a]

matrix	σ (Å)	ϵ (cm^{-1})	$\hat{\epsilon}$ (cm^{-1})	ρ (Å^{-3})	$\hat{\rho}$ (Å^{-3})	ρ_{cryst} (Å^{-3})
argon	3.405	1.57	23.1	0.145	0.009 75	0.0267
krypton	3.65	2.45	33.4	0.104	0.007 87	0.0222
xenon	3.98	4.58	47.5	0.062	0.005 94	0.0173

[a] Also listed are the Lennard-Jones parameters σ and the number density ρ_{cryst} found in rare gas crystals.[26]

(fwhm) Γ_s, and the solvent shift $\nu_s(Q_x)$ with respect to the gas-phase absorption of H_2Pc.[28]

According to the statistical mechanical model outlined above, the inhomogeneously broadened absorption band is expected to have a Gaussian shape. However, the measured absorption bands show a slight asymmetry on the low-energy side. This observation indicates a second preferential position of phthalocyanine in rare gas matrices, which had been noticed earlier in argon.[29] Indeed, the argon absorption band can be reproduced well by two Gaussians shifted with respect to each other by 70 cm^{-1}. The correction hardly alters the parameters of the dominant band (given in Table 1), which were obtained with a single Gaussian fit, and is therefore omitted in the following.

The observed increase of the solvent shift ν_s from argon to xenon matrices implies an increased interaction between guest molecule and host matrix. This is due to the increasing matrix polarizability, which is strong enough to compensate for the decreasing number of matrix atoms within the interaction range of the guest molecule (essentially limited to three solvent shells[24]). Therefore, when going from argon to xenon, fewer matrix units produce the increasing solvent shift. According to basic statistics, the relative fluctuations of the number of rare gas atoms interacting with the guest molecules increase as well,[30] which finds its expression in larger fluctuations of the transition energy shifts of H_2Pc. Therefore, we expect an increasing inhomogeneous width Γ_s, which is observed (see Table 1).

We now apply the statistical model to extract from the measured values of ν_s and Γ_s the number density ρ of matrix units surrounding the guest molecule and the interaction potential parameter ϵ with and without consideration of matrix correlations. First, the parameters σ, R_c, and R_0 have to be specified. From literature data for σ (see Table 2, taken from ref 26), R_c can be calculated. As guest−molecule radius R_F, which is needed to calculate R_0, we take the radius along the long in-plane axis of H_2-Pc: $R_F = 6.5$ Å.[31] At this point we want to reemphasize that, in polymeric host matrices, the geometrical parameters R_0, R_c, and σ are not known due to the complexity of the matrix units in these systems. These parameters had to be calculated using additional input data such as the pressure-induced shift of spectral holes. Since these parameters are known for solid rare gases, the measured inhomogeneous line shapes are sufficient to extract number densities and interaction potential parameters with ($\hat{\rho}$,$\hat{\epsilon}$) and without (ρ,ϵ) consideration of matrix correlations. The results are summarized in Table 2.

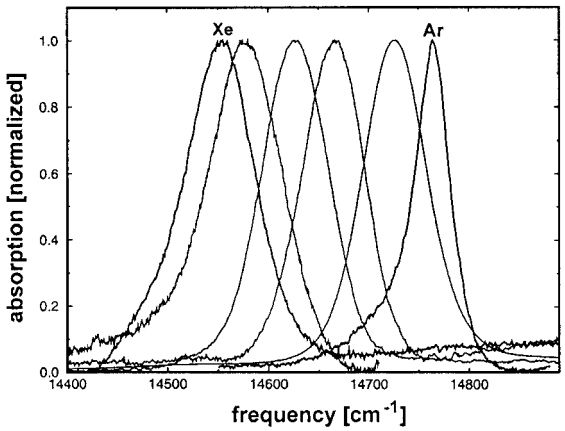

FIGURE 2. Normalized absorption spectra of the Q_x band of H_2Pc in solid $Ar_{1-x}Xe_x$ matrices. From left to right: $x = 1$ (pure Xe), $x =$ 0.6, 0.4, 0.3, 0.15, $x = 0$ (pure Ar).

Comparing the calculated number density ρ to the number density ρ_{cryst} found in rare gas crystals shows that, without consideration of matrix correlations, the statistical model yields physically unrealistic matrix densities, which are almost half an order of magnitude larger than the densities observed for single crystals! Moreover, this overestimation of the number density results in interaction potential parameters ϵ that are too small to account for the observed solvent shift, as a simple shell structure model quickly verifies.[24] These results show that the low-density approximation $\rho \rightarrow 0$ (see section 2) used in earlier studies is questionable. When matrix correlations are taken into account as sketched in section 2, the number density $\hat{\rho}$ drops far below ρ_{cryst}, and the depth of the dye−matrix interaction potential $\hat{\epsilon}$ increases accordingly (see Table 2). Since $\hat{\epsilon}$ represents the solvent shift of one matrix unit located in the minimum of the transition energy shift function (eq 2), its value can be compared to the solvent shifts found in clusters of aromatic molecules with just one attached rare gas atom:[32,33] for various aromatics, the first attached rare gas atom provides about 8% of the total shift. For our systems, the ratio $\hat{\epsilon}/\nu_s$ is between 6.3% and 8%, confirming the reliability of the results. Therefore, to obtain physically reasonable results, matrix correlations have to be included. As mentioned above, the calculated number densities $\hat{\rho}$ are significantly below the crystalline number densities ρ_{cryst}, implying that H_2Pc is located in a low-density region of the nanocrystalline sample. These data therefore support the notion that the guest molecule is located in the interstitial regions between the grains.

Quench-condensed $Ar_{1-x}Xe_x$ mixtures are amorphous for $0.2 < x < 0.7$ and nanocrystalline otherwise.[17] To study whether these structural differences affect the inhomogeneous line shape, we studied H_2Pc-doped $Ar_{1-x}Xe_x$ mixtures. Figure 2 shows the inhomogeneous Q_x absorption band of H_2Pc-doped argon−xenon matrices for different mixing ratios. The Q_x band has a Gaussian shape, with the band maximum located between the band maxima of the two constituents. The band shape cannot be described as a superposition of pure argon and xenon spectra, which demonstrates that the gases are homogeneously mixed during the condensation process and also

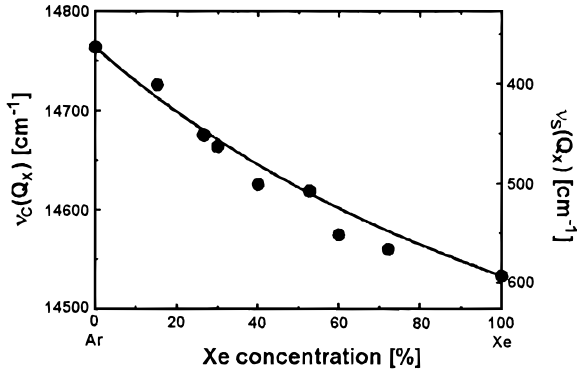

FIGURE 3. Position of the maximum of the Q_x band (left-hand scale) and solvent shift ν_s (right-hand scale) of H_2Pc in $Ar_{1-x}Xe_x$ matrices versus Xe concentration.

in the solid matrix. As in pure rare gas matrices, the mean matrix−dye interaction manifests itself in the frequency of the absorption band maximum, which for the rare gas mixtures is plotted in Figure 3 versus the Xe concentration. The right scale displays the solvent shift, which increases continuously with increasing Xe concentration. The solid line in Figure 3 is derived from eq 4, which was extended to mixed systems. The density of the matrix was interpolated between the values of the pure components as described in ref 34. Given this simple approach, the agreement of the calculated curve with the experimental data is quite satisfactory.[35]

Due to the limited range of the dispersive guest/host interaction, only the local environment of H_2Pc determines the solvent shift. From the continuously increasing solvent shift with increasing Xe concentration, we may conclude that the local environment also changes continuously over the entire composition ratio and that no drastic change of the number density of matrix units within the interaction range of the guest molecule takes place. This corroborates the notion that the local environment of H_2Pc is noncrystalline already in pure rare gas hosts.

5. Pressure Effects

The application of hydrostatic pressure induces positional changes of the matrix units from their "equilibrium" positions, which makes it possible to modify the guest−matrix interaction strength in a controlled fashion. The modified guest−matrix interaction strength leads, in turn, to a shift of the electronic transition energy. Experimentally, we measure this line shift by recording the changes of a spectral hole when hydrostatic pressure is applied. Using the statistical model described in section 2, from the shift of the center of the spectral hole the compressibility of the matrix surrounding the guest molecule is calculated.

We have seen that consideration of matrix correlations greatly influences the results for the microscopic interaction parameter ϵ and the number density ρ. The question arises of whether matrix correlations play an equally prominent role in the determination of matrix compressibilities. It was mentioned earlier that, for the case of a purely attractive van der Waals potential, the equation describing the pressure-induced shift of the hole center (eq 12) remains unchanged when matrix correlations are introduced, implying that matrix correlations do not affect the result for the compressibility. Furthermore, the analysis of the pressure-induced hole shifts in polymer hosts using eq 12 (for $\Delta T = 0$ K) yields compressibilities that agree quite well with mechanically determined values.[9] To determine whether this apparent insignificance of matrix correlations for the hole shifts also holds if the transition energy shift function (eq 2) is used, the pressure-induced hole shift with and without consideration of correlations is now analyzed numerically.

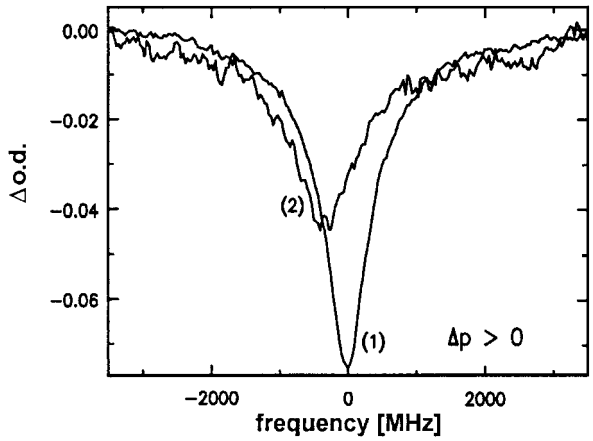

FIGURE 4. Pressure shift and broadening of a spectral hole (H_2Pc in Ar). Trace 1, original hole profile; trace 2, spectral hole after a pressure increase of 88 kPa.

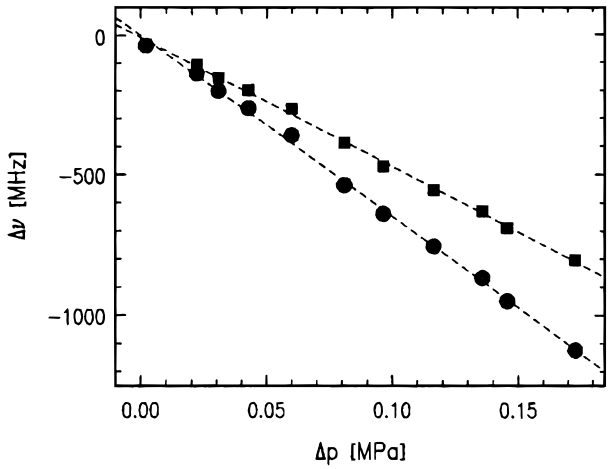

FIGURE 5. Shift of hole center vs pressure change: raw data (■) and data after temperature correction (●).

Figure 4 shows the changes of a spectral hole in an argon matrix due to an increase of pressure and temperature. While retaining a Lorentzian profile, the position of the hole center shifts to a lower frequency and the hole broadens. The measured shift of the hole center is plotted in Figure 5 (squares) versus the pressure increase, although the shift is also due to the concomitant temperature increase. The circles in Figure 5 show the pure pressure effect after the contribution of the thermal expansion of the matrix has been removed as outlined in section 2 (see ref 24). From the corrected data, the

Table 3. Matrix Compressibilities Determined with ($\hat{\kappa}$) and without (κ) Correlations, Using Lennard-Jones (LJ) and van der Waals (vdW) Potentials[a]

matrix	κ_{vdW} (Gpa^{-1})	κ_{LJ} (GPa^{-1})	$\hat{\kappa}_{LJ}$ (GPa^{-1})	κ_{cryst} (GPa^{-1})
argon	0.28	0.24	0.25	0.35
krypton	0.29	0.27	0.29	0.30
xenon	0.42	0.39	0.38	0.27

[a] The crystalline compressibilities κ_{cryst} are taken from ref 36.

compressibility was determined numerically. The results are listed in Table 3. Comparing columns 2 and 3 reveals that the calculated compressibilities with ($\hat{\kappa}_{LJ}$) and without (κ_{LJ}) correlations are identical within the experimental accuracy. This confirms that, for the determination of compressibilities, matrix correlations are of no importance! Moreover, the compressibilities hardly change if the full Lennard-Jones-based shift function (eq 2) is approximated by the simple van der Waals potential (κ_{LJ} versus κ_{vdW} in Table 3), suggesting that the interacting matrix units are located within the attractive part of the Lennard-Jones interaction potential. This interesting result justifies the widespread use of the analytical expression (eq 12)[6–8] for compressibility determinations in a variety of samples. We would like to emphasize that this proof was possible only by the use of rare gases as host matrices, where the geometrical parameters of the matrix units are well defined!

The compressibilities κ_{cryst} of large, pure rare gas crystals[36] decrease from argon to xenon, which is due to the increasing strength of the van der Waals interaction. This behavior is opposite to that found in our systems. Since the guest/host interaction parameters are the same as those in bulk crystals, the discrepancy has to have a structural origin. For example, the higher compressibility of a xenon matrix around H_2Pc can be explained by larger free volume, which is equivalent with a smaller number density ρ as compared to the bulk (see section 4). In this light, the numbers for argon remain puzzling: one could speculate that in argon the large number of randomly oriented, interlocking crystallites shield the guest molecule to some extent, leading to an "effective" pressure at the guest site that is smaller than the externally applied pressure. At this point, no definite conclusion is possible. However, our data support the notion that the local environment of H_2Pc is noncrystalline.

6. Homogeneous Line Shapes

As discussed in the Introduction, dynamical scattering processes involving lattice vibrations and (pseudo) local models are reflected in the homogeneous line shape. Amorphous samples contain additional low-energy excitations—described as two-level tunneling systems (TLS)—which are not found in ideal crystals. Therefore, the homogeneous line shape also contains structural information. Putting identical guest molecules in two different phases should result in markedly different homogeneous widths.[13] We investigated this aspect by measuring the homogeneous line widths at the center of the absorption band. Figure 6 shows the measured widths vs the Xe concentration. In pure argon matrices, the homogeneous line width is significantly smaller than that in pure xenon. It gradually increases up to a Xe concentration of 50%, with no recognizable discontinuity at the expected transition from a polycrystalline to an amorphous structure. From specific heat experiments[17] it is known that low-energy excitations such as TLS and pseudo-local modes are present not only in the amorphous phase but also in pure solid rare gases, where these excitations can exist in phase boundaries and in the neighborhood of impurities inside the crystallites. The lack of a sudden change of the homogeneous line width at the transition to the amorphous phase may therefore be attributed to the high disorder and porous structure, which is characteristic for pure quench-condensed matrices.

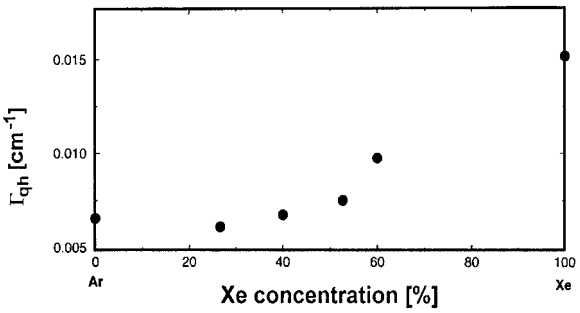

FIGURE 6. Homogeneous line widths at the maximum of the Q_x band of H_2Pc in $Ar_{1-x}Xe_x$ matrices versus Xe concentration, $T = 1.8$ K.

Further evidence for the assumption that H_2Pc is located in the disordered interstitial regions between the crystallites of pure rare gas solids comes from the observation that the homogeneous line widths of H_2Pc in pure rare gases are comparable to those of H_2Pc in amorphous polymers and significantly larger than those of *tert*-butyl H_2Pc in a crystalline *n*-hexadecane matrix.[13] Therefore, H_2-Pc is not located in a crystalline local environment in pure solid rare gases.

7. Summary

We applied a statistical mechanical model describing the inhomogeneous broadening of electronic transitions of guest molecules in solid hosts. This model also accounts for the pressure-induced changes of spectral holes burnt in these transitions. Inherent in this model is the dissection of the host material in spherical matrix units that interact independently and only dispersively with the guest molecules. Initially this model was applied to polymeric hosts, in which case the concept of individual and independent matrix units was questionable. Therefore, we studied solid rare gas hosts, which are ideal systems with regard to the assumptions made in the model. The simplicity of rare gases provided readily geometrical parameters that were not available for polymer hosts.

Our systematic studies of the model using rare gas hosts proved that the consideration of correlations between matrix units is crucial for the extraction of physically reasonable microscopic interaction parameters (e.g., mini-

mum value of transition energy shift function) from measured inhomogeneous line shapes. Furthermore, in combination with the measured homogeneous line widths of guest molecules in pure and mixed solid rare gases, these data provided structural information on the local environment of the guest molecule: we verified that in quench-condensed, pure rare gases the guest molecule is located in low-density regions between the crystallites of the host matrix. Further evidence for this assignment comes from the calculated compressibilities. Interestingly, matrix correlations are of little importance for the determination of matrix compressibilities from pressure-shifted spectral holes.

We gratefully acknowledge many stimulating discussions with Dr. L. Kador.

References

(1) Geissinger, P.; Kohler, B. E.; Kulikov, S. G.; Terpougov, V. Inhomogeneous Broadening of Electronic Spectra in Organic Model Systems. *J. Chem. Phys.* **1998**, *108*, 1821−1829.

(2) Hayes, J. M.; Small, G. M. Non-Photochemical Hole-Burning and Impurity Site Relaxation Processes in Organic Glasses. *Chem. Phys.* **1978**, *27*, 151−157.

(3) Hsu, D.; Skinner, J. L. Nonperturbative Theory of Temperature-Dependent Optical Dephasing in Crystals. IV. Microscopic Model for Pseudolocal Phonons. *J. Chem. Phys.* **1987**, *87*, 54−59.

(4) Stoneham, A. M. Shapes of Inhomogeneously Broadened Resonance Lines in Solids. *Rev. Mod. Phys.* **1969**, *41*, 82−108.

(5) Laird, B. B.; Skinner, J. L. On the Microscopic Nature of Inhomogeneously Broadened Spectra of Chromophores in Glasses and Crystals. *J. Chem. Phys.* **1989**, *90*, 3880−3881.

(6) Pschierer, H.; Friedrich, J.; Falk, H.; Schmitzberger, W. Molecular Interactions and Correlation Phenomena between Pressure Shift and Solvent Shift: A Spectral Hole-Burning Study. *J. Phys. Chem.* **1993**, *97*, 6902−6906.

(7) Zollfrank, J.; Friedrich, J.; Parak, F. Spectral Hole-Burning Study of Protoporphyrin IX Substituted Myoglobin. *Biophys. J.* **1992**, *61*, 716−724.

(8) Reul, S.; Richter, W.; Haarer, D. Spectral Hole Burning in H_2Pc-doped Silica Aerogels. *J. Non-Cryst. Solids* **1992**, *145*, 149−153.

(9) Laird, B. B.; Skinner, J. L. Microscopic Theory of Reversible Pressure Broadening in Hole-Burning Spectra of Impurities in Glasses. *J. Chem. Phys.* **1989**, *90*, 3274−3281.

(10) Hornig, L.; Schnur, N.; Weiss, G.; Hunklinger, S. Acoustic Measurements on Vapour Condensed Xe-films. *Phys. Lett. A* **1988**, *132*, 55−58.

(11) Gleiter, H. Nanostructured Materials. *Adv. Mater.* **1992**, *2*, 474−481.

(12) Zhu, X.; Birringer, R.; Herr, U.; Gleiter, H. X-ray Diffraction Studies of the Structure of Nanometer-Sized Crystalline Materials. *Phys. Rev. B* **1987**, *35*, 9085−9090.

(13) Geissinger, P.; Reul, S.; Haarer, D.; Rieckhoff, K. E. Hole-Burning in the Amorphous and in the Crystalline Local Environment of an N-Hexadecane Shpolskii Matrix. *Chem. Phys. Lett.* **1992**, *190*, 67−71.

(14) Kador, L.; Schulte, G.; Haarer, D. Relation between Hole-Burning Parameters and Molecular Parameters: Free-Base Phthalocyanine in Polymer Hosts. *J. Chem. Phys.* **1986**, *90*, 1264−1270.

(15) Sesselmann, T.; Richter, W.; Haarer, D. Correlation Between Pressure-Induced Optical Shifts and Compressibilities of Polymers Doped with Dye Molecules. *Europhys. Lett.* **1986**, *2*, 947−952.

(16) Reul, S.; Richter, W.; Haarer, D. Spectroscopic Studies of the Solute−Solvent Interaction in Dye-Doped Polymers: Frequency-Dependent Pressure Shifts. *Chem. Phys. Lett.* **1991**, *180*, 1−5.

(17) Menges, H.; Löhneysen, H. v. Specific Heat of Disordered and Amorphous Rare-Gas Solids: Quench-Condensed Pure and Binary Films. *J. Low Temp. Phys.* **1991**, *84*, 237−260.

(18) Kharlamov, B.; Personov, R.; Bykovskaja, L. Stable Gap in Absorption Spectra of Solid Solutions of Organic Molecules by Laser Irradiation. *Opt. Commun.* **1974**, 191−193.

(19) Gorokhovskiĭ, A.; Kaarli, R.; Rebane, L. Burnout of the Dip in the Contour of a Purely Electron Line in Shpolskii Systems. *JETP Lett.* **1974**, *20*, 216−218.

(20) Friedrich, J.; Haarer, D. Photochemical Hole-Burning: A Spectroscopic Study of Relaxation Processes in Polymers and Glasses. *Angew. Chem., Int. Ed. Engl.* **1984**, *23*, 113−140.

(21) Markoff, A. *Wahrscheinlichkeitsrechnung*; Teubner: Leipzig, 1912.

(22) Simon, S. H.; Dobrosavljevic, V.; Stratt, R. M. The Local Field Distribution In A Fluid. *J. Chem. Phys.* **1990**, *93*, 2640−2657.

(23) Sevian, H. M.; Skinner, J. L. A Molecular Theory of Inhomogeneous Broadening, Including the Correlation Between Different Transitions, in Liquids and Glasses. *Theor. Chim. Acta* **1992**, *82*, 29−46.

(24) Geissinger, P.; Kador, L.; Haarer, D. Importance of Matrix Correlations in Dye-Doped Solid Rare Gases: A Hole-Burning Study. *Phys. Rev. B* **1996**, *53*, 4356−4366.

(25) Haymet, A. D. J. Orientational Environments and High Order Correlation Functions in Liquids. *J. Phys. (Paris) Coll.* **1985**, *46*, C9−27.

(26) Horton, G. Ideal Rare-Gas Crystals. *Am. J. Phys.* **1968**, *36*, 93−119.

(27) Geissinger, P.; Haarer, D. Hole-burning in Dye-Doped Rare-Gas Matrices. *Chem. Phys. Lett.* **1992**, *197*, 175−180.

(28) Fitch, P. S. H.; Haynam, C. A.; Levy, D. H. The Fluorescence Excitation Spectrum of Free Base Phthalocyanine Cooled in a Supersonic Free Jet. *J. Chem. Phys.* **1978**, *73*, 1064−1072.

(29) Bondybey, V. E.; English, J. H. Spectra of the H2-Phthalocyanine in Low-Temperature Matrices. *J. Am. Chem. Soc.* **1979**, *101*, 3446−3450.

(30) Kador, L. Stochastic Theory of Inhomogeneous Spectroscopic Line Shapes Reinvestigated. *J. Chem. Phys.* **1991**, *95*, 5574−5581.

(31) Chen, I. Molecular Orbitals of Phthalocyanine. *J. Mol. Spectrosc.* **1967**, *23*, 131−143.

(32) Leutwyler, S.; Even, U.; Jortner, J. Resonant Two-Photon Ionization of Fluorene Rare-Gas van der Waals Complexes. *J. Chem. Phys.* **1983**, *79*, 5769−5779.

(33) Ben-Horin, N.; Banhatt, D.; Even, U.; Jortner, J. Spectroscopic Interrogation of Heterocluster Isomerization II. *J. Chem. Phys.* **1992**, *97*, 76011−6031.

(34) Loistl, M.; Baumann, F. Refractive Index and Mass Density of Quench Condensed Argon−Xenon Films. *Z. Phys. B−Condensed Matter* **1991**, *82*, 199−203.

(35) Giering, T.; Geissinger, P.; Kador, L.; Haarer, D. Persistent Spectral Hole Burning in Dye-Doped Quench Condensed Argon−Xenon Matrices. *J. Luminesc.* **1995**, *64*, 245−251.

(36) Anderson, M. S.; Swenson, C. A. Experimental Equations of State for the Rare Gas Solids. *J. Phys. Chem. Solids* **1975**, *36*, 145−162.

AR980011L